

# 648 Appendix

## 649 A Agent Structure

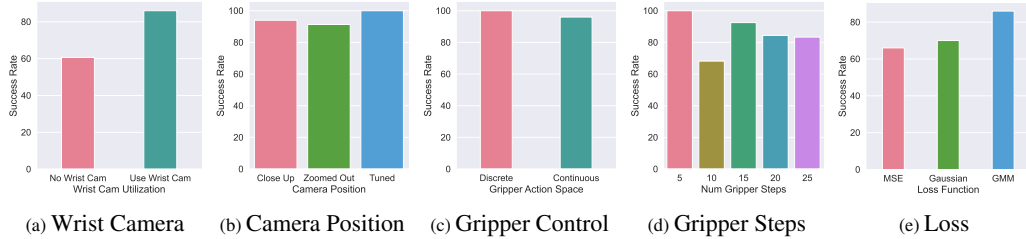


Figure A.1: **Effect of Observation, Action and Loss Decisions.** We ablate a variety of design decisions in OPTIMUS and demonstrate that each produces a clear improvement.

650 **Observation spaces:** We use the same set of proprioceptive observations across all tasks: end-effector  
651 position, end-effector orientation (quaternion), gripper position. For each task, we select a different  
652 camera view that maximizes scene coverage. For Shelf and Microwave, we use two views, left  
653 and right shoulder views, whereas for the rest of the tasks we use a single forward facing view.  
654 Additionally, we use a wrist camera for every task, which greatly improves the performance. We use  
655 camera images of size 84x84. We empirically validate these decisions in Sec. B.1 and visualize the  
656 results in Fig. A.1.

657 **Action spaces:** As mentioned in the main text, we use task space control for moving the arm.  
658 In Robosuite, we use the built-in OSC controller [59]. In IsaacGym, we used a simple IK-based  
659 task-space controller. With regard to gripper control, we discuss and resolve two challenges related  
660 to TAMP. 1) Continuous gripper actions produced by the TAMP solver can be challenging for the  
661 network to fit, as the network does not fully commit to predicting grasps. To that end, we modify  
662 the gripper actions to be binary open and close motions which improves performance and reduces  
663 noise in policy execution. We validate that this results in a performance improvement in Sec. B.1.  
664 2) TAMP demonstrations can include “stall regions”: segments of the trajectory in which the robot  
665 is not moving, such as when TAMP executes gripper-only actions for grasps and placements. This  
666 results in trained policies that may freeze after grasping an object, as the data does not contain cues  
667 for when to exit the stall region. To address this issue, we tune the length of stall regions during data  
668 collection against the agent’s history length to ensure data collection success rate remains high while  
669 minimizing policy freezing behavior.

670 **B Additional Learning Results**

671 **OPTIMUS can learn to adapt its behavior based on the scene configuration.** We evaluate  
 672 OPTIMUS on two tasks that involve adapting the task plan based on the configuration of objects in  
 673 the scene: StackAdapt and MicrowaveAdapt, and two that require adapting motions to randomized  
 674 receptacle sizes: ShelfReceptacle and MicrowaveReceptacle. As shown in Table B.1, OPTIMUS  
 675 is able to effectively leverage visual input to learn when additional stacking operations are needed  
 676 (StackAdapt) or when the area in front of the microwave needs to be cleared (MicrowaveAdapt),  
 677 achieving 96% and 75% respectively, compared to the best baseline (96% and 40%). Additionally,  
 678 we demonstrate that OPTIMUS is able to effectively learn to generalize to unseen receptacle sizes  
 679 with high success rates, achieves 80% and 70% on held out shelves and microwaves respectively.  
 680 These results illustrate that OPTIMUS can distill scene conditioned task plan adaptation and motion  
 681 generalization across scene configurations from TAMP supervision.

Dataset	BC-MLP	BC-RNN	BeT	OPTIMUS
StackAdapt	96	92	81	96
MicrowaveAdapt	25	40	13	75
ShelfReceptacle	72	71	59	80
MicrowaveReceptacle	48	55	31	70

Table B.1: **Scene-based adaptation results.** OPTIMUS can learn to vary the task plan it executes based on the scene configuration (*rows 1 and 2*) as well as adapt to unseen receptacles (*rows 3 and 4*).

682 We describe and empirically validate three advantages of the distilled policies over the TAMP  
 683 system: 1) success rate improvement over the TAMP supervisor, 2) faster run-time, 3) operation from  
 684 perceptual instead of state input.

685 **OPTIMUS almost doubles the performance of the TAMP supervisor.** To evaluate TAMP, we  
 686 execute 50 trials averaged over three random seeds on each single-task environment and record the  
 687 performance in Table B.2. We find that OPTIMUS is able to outperform the TAMP system by a wide  
 688 margin, from 20% on the easiest task, PickPlace, to 64% on Microwave-1 and 44% on the hardest  
 689 task, PickPlaceFour. TAMP with joint space control has better performance on average than TAMP  
 690 with task space control (52% vs. 45%), but still performs significantly worse than OPTIMUS (52%  
 691 vs. 87%). We instead find that not all grasps execute perfectly every time, likely due to differences in  
 692 simulation, planning and control schemes from the ACRONYM paper. As a result, we observe grasp  
 693 execution failures and object slippage during placement motions. OPTIMUS avoids learning these  
 694 failure cases by only distilling the successful trajectories, which enables it to successfully generalize  
 to unseen configurations of the task.

Dataset	TAMP-joint	TAMP-task	OPTIMUS
PickPlace-1	82	82	100
PickPlaceTwo	52	58	96
PickPlaceThree	40	50	91
PickPlaceFour	34	16	60
Shelf-1	58	44	91
Microwave-1	46	22	86
Average	52	45	87

Table B.2: **Comparison of OPTIMUS vs. TAMP.** We plot percentage success on randomly chosen states from the environment. We find OPTIMUS greatly outperforms the TAMP supervisor, whether TAMP uses task space control or joint space.

695  
 696 **OPTIMUS executes 5-7.5x faster than TAMP.** We evaluate the run-time of OPTIMUS against  
 697 TAMP by computing the average time per step for both systems across 100 trials. We run the  
 698 evaluation on a machine with an RTX 3090 GPU and Intel i9-10980XE CPU and include the results  
 699 in Table B.3. TAMP takes 0.15s per action on average while OPTIMUS (30M parameters) takes  
 700 0.021s per action and OPTIMUS (100M parameters) takes 0.031s per action. TAMP pays a high  
 701 up-front cost of 2-5 seconds, and then executes a feedback controller to quickly track the planned  
 702 way-points. In contrast, OPTIMUS spends a constant amount of time per action. Furthermore, it is  
 703 possible to greatly improve the inference time performance of OPTIMUS by employing techniques  
 704 such as FlashAttention [70], model compilation, and TensorRT.

TAMP	OPTIMUS (30M)	OPTIMUS (100M)
.15s	.021s	.031s

Table B.3: **Timing Results.** We measure the average time taken per action (lower is better). On average, OPTIMUS is 5-7.5x faster to execute than TAMP.

705 **By distilling TAMP, we obtain a performant policy that executes high-frequency *low-level***  
706 **control from *purely perceptual* input.** OPTIMUS produces policies that are fast to execute, reactive  
707 and perform visuomotor control at similar performance to policies that have access to state information  
708 (Fig. A.1) and out-performs the privileged TAMP expert (Table B.2).

## 709 B.1 Ablations

710 In this section, we ablate additional components of OPTIMUS, namely the gripper control scheme  
711 and data generation process, observation space design and loss function.

712 **Discrete gripper control and short "stall" regions directly impact the performance of TAMP**  
713 **imitation.** We first analyze the impact of switching from continuous to discrete gripper control on  
714 the Stack task in Fig. A.1. By using discrete control, we can improve the success rate by 4%, while  
715 qualitatively we observe smoother gripper control and decisive grasps. On the other hand, we find  
716 that the decision to tune the length of "stall" regions, namely TAMP grasp and release actions, is  
717 crucial to the performance of OPTIMUS. As observed in Fig. A.1, reducing the number of control  
718 actions per grasp and release action greatly improves performance, from 78% at 25 steps to 100% at 5  
719 actions. This is likely due to two reasons, 1) we shorten the overall length of the roll-outs, easing the  
720 learning burden, and 2) we reduce the likelihood of the policy to encounter a series of states where  
721 the observations and actions do not change, which can result in freezing behavior in the policy.

722 **Camera view selection enables greatly improved visuomotor learning.** We evaluate two camera  
723 views on the Stack task. Both camera poses keep all objects as well as the robot in view; one is  
724 close up which hinders accurate estimation of scene geometry while the other is farther away which  
725 decreases the size of the objects in the frame, making it difficult for the policy to focus on them. As a  
726 result, we find in Fig. A.1 that a well-tuned camera view that is angled and positioned appropriately  
727 performs best. We additionally evaluate the impact of using a wrist camera. For tasks with primitive  
728 objects such as blocks, we found that the wrist cam had little impact. However, moving to tasks such  
729 as Microwave, where close up views of the handle and target object enable improved perception of  
730 grasp geometries, the wrist camera affords a significant performance improvement as we show in  
731 Fig. A.1.

732 **GMM loss enables OPTIMUS to better handle the multi-modality of TAMP supervision.** TAMP  
733 generates highly multi-modal action distributions through randomized planning and non-deterministic  
734 IK. Therefore, as we note in Sec. 3.3, we use Gaussian Mixture Models to model the multi-modality.  
735 We experimentally validate that GMM output distributions greatly improve learning performance  
736 by comparing against MSE loss, which produces a deterministic, uni-modal output distribution,  
737 and Gaussian log-likelihood, which produces a non-deterministic, uni-modal output distribution.  
738 We find that GMM loss greatly out-performs both output distributions (86% vs. 66% and 70%).  
739 While including a stochastic output distribution such as a Gaussian does improve performance by  
740 4%, the multi-modality of GMM produces a further improvement of 16% performance. The results  
741 demonstrate that by providing the policy a more expressive output distribution, we can greatly  
742 improve how well the policy can model the TAMP expert.

## 743 C Environments

744 In this section, we provide a detailed description of the environments we use to evaluate OPTIMUS.  
745 We begin by describing settings which are common across environments. We then discuss each task  
746 individually.

747 For all tasks, we use a Franka Panda 7-DOF manipulator with the default Franka gripper, though the  
748 TAMP system is capable of generating supervision using any manipulator, provided the robot URDF.  
749 For the Stack task, we use the block stacking environment from Robosuite [58], modifying it to  
750 include up to 5 blocks and a larger workspace region. For all other tasks we use IsaacGym [71] with  
751 the PhysX [72] back-end. For each task, we use a fixed reset pose for the robot, while randomizing  
752 the positions of sampled objects. Object orientation about the z-axis is sampled uniformly at random  
753 from 0 to 360 degrees for all tasks.

754 For PickPlace, Multi-step PickPlace, Shelf and Microwave, we sample objects from ShapeNet [49].  
755 We select objects that have valid grasps in the Acronym [51] dataset. We further refine our dataset by  
756 filtering out objects that do not simulate well in our IsaacGym environments. From the remaining  
757 objects, we form two datasets with 19 and 72 objects respectively.

758 We next provide additional details for each task.

759 **Stack:** The goal is to stack the blocks in a fixed ordering. Each block is a different color. The block  
760 positions are sampled uniformly in an area of size 28cm x 28cm. The base block is of size  $2.5cm^3$ ;  
761 the rest are of size  $2cm^3$ . The task is considered solved if all of the blocks are stacked in the correct  
762 ordering.

763 **StackAdapt:** The task is the same as Stack, except there are two platforms, the blocks must be  
764 stacked on the target platform only. There is a 50/50 chance for the base block to be spawned on the  
765 target platform, in which the task simply involves stacking, and the base block to be spawned on the  
766 other platform, which requires the agent to first place the base block on the target platform then stack  
767 on top of it.

768 **PickPlace:** The task involves picking and placing ShapeNet objects from the left platform to the  
769 right platform. The platforms are of size .25 by .25 and are kept .5 apart. The object positions are  
770 sampled uniformly at random on the platform. The task success criteria is fulfilled if the object is  
771 placed anywhere on the target platform.

772 **Multi-step PickPlace:** The task involves picking and placing ShapeNet objects from platforms on  
773 the left to bins on the right. Up to four objects: a basket, vase, magnet or cup are sampled on separate  
774 platforms. Each platform is of size .15x.15 and each bin is of size .2x.2m. Each object's position is  
775 sampled uniformly at random on its associated platform. The task is solved when all objects are in  
776 their associated bins.

777 **Shelf:** The task involves moving ShapeNet objects from the lower rung of the shelf to the middle  
778 one. The shelf is 1m tall and has three rungs of size .5m x .25. The position and size of the shelf are  
779 constant. Object positions are sampled on the lowest rung, uniformly at random across the surface.  
780 The task is solved when the object is placed on the middle rung.

781 **ShelfReceptacle:** This task is the same as Shelf, but the shelf size is randomized within the following  
782 intervals: height (.8-1m), rungs: (.5x.25m - .4x.75m).

783 **Microwave:** The goal is to open the microwave by pulling open the handle, grasp a ShapeNet object,  
784 and place it inside the microwave. The microwave is .3m tall, 50cm wide and 20 cm deep. Microwave  
785 position and size are held fixed. The initial angle of the microwave door is 0, i.e. fully closed. Object  
786 positions are sampled on a platform of size .25x.25m. The agent has succeeded when the object is  
787 inside the microwave.

788 **MicrowaveReceptacle:** This task is the same as Microwave, but the microwave size is randomized  
789 within the following intervals: height (.3-.4m), width: (.5-.6m), depth: (.2-.3m).

790 **MicrowaveAdapt:** The task is the same as the microwave task, except with 50% probability an  
791 object is spawned in front of the microwave door, requiring the agent to first move the object aside  
792 then open the door and place the target object inside.

Hyper-parameter	Value
Learning Rate	0.0001
Batch Size	16/512
Warmup Steps	0
Linear Scheduling Steps	100K
Final Learning Rate	0.00001
Weight Decay	0.01
Gradient Clip Threshold	1.0
Number of Gradient Steps	1M
Optimizer Type	AdamW
Loss Type	GMM
GMM Components	5
GMM Min. Std. Dev.	0.0001
GMM Std. Dev. Activation Fn.	SoftPlus

Table D.1: Hyper-parameters used during training.

	OPTIMUS (30M/100M)	MLP (30M/100M)	RNN (30M/100M)	BeT (30M/100M)
Num Layers	6/12	2/6	2/3	6/12
Hidden Dimension		1024/1024	1000/2000	
Context Length	8/8		10/10	10/10
Num Heads	8/16			8/16
Transformer Embed. Dim.	256/512			256/512
Embedding Dropout Prob.	0.1/0.1			0.1/0.1
Attention Dropout Prob.	0.1/0.1			0.1/0.1
Output Dropout Prob.	0.1/0.1			0.1/0.1
Positional Embed.	Learned/Learned			Learned/Learned
Positional Embed. Type	Relative/Relative			Relative/Relative
Num. Clusters				24/24
Offset Loss Scale				100/100

Table D.2: Model hyper-parameters.

794 **Network and Training Details:** We include the model hyper-parameters for the 30M and 100M  
795 parameter variants of each method in Table D.2. For the vision-backbone, as discussed in the main  
796 text, we use a Resnet-18 [60] with a Spatial Softmax [61] output to encode each image separately.  
797 For details, please see the Robomimic paper [29]. We include learned positional embeddings with  
798 each token and employ relative, rather than absolute, position embeddings to enable the network to  
799 adapt to longer horizons at test time. We use a linear annealing schedule that reduces the learning rate  
800 from  $10^{-4}$  to  $10^{-5}$  over 100K gradient steps and then keeps the learning rate constant. We train with  
801 the AdamW optimizer with a weight decay of 0.01 and no learning rate warm-up. For single-task  
802 learning, we train with a batch size of 16 on a single V100 GPU, while for multi-task learning we  
803 train using batch size of 512 to 1024 depending on the task, across 8 V100 GPUs. For visuomotor  
804 learning, we train with multiple camera views with image size 84x84, and we augment the data with  
805 random crops [29, 73, 74]. We additionally list the hyper-parameters used for training in Table D.1.  
806 One note of interest: for multi-task training, we found that increasing the batch size greatly improved  
807 the results; hence we use a batch size of 512.

808 For BeT, we tried using the original authors codebase, which we augmented with our vision backbone,  
809 but found that the performance was extremely low. Instead, we re-implemented BeT as a modification  
810 of OPTIMUS, using the same network structure but predicting a discrete cluster center and offset  
811 head instead and training using the focal and MT losses from the BeT paper. We found that the  
812 standard hyper-parameters for BeT did not perform well, and after significant hyper-parameter tuning  
813 found that the combination of 24 cluster centers and offset loss scale of 100 performed best.

814 **Evaluation Protocol:** We note additional details regarding our evaluation protocol as follows. We  
815 split each dataset into a set of training and validation trajectories (using a 90/10 split). From the  
816 validation trajectories, we save the initial state of the demonstration. During evaluation, we reset  
817 the simulator state to an initial state from the validation set, and execute the policy from there. By  
818 comparing on the same set of validation states, we can better evaluate performance across seeds and  
819 algorithms. Note this means evaluation is performed from states that the TAMP solver is able to  
820 solve. As we note in Sec. 4.1, in practice this distinction matters little, as the TAMP system does not  
821 have a systematic failure case which could be passed on to the policy. Therefore we observe similar  
822 success rates when evaluating on randomly sample poses from the environment.

## 823 E Related Work

### 824 E.1 Offline Learning from Demonstrations

825 Imitation Learning (IL) is a paradigm for training robots to perform manipulation tasks by leveraging  
826 a set of expert demonstrations. In this work, we focus on offline learning, in which a policy learns  
827 a dataset of demonstrations, without any additional interaction. This is typically done through  
828 Behavior Cloning (BC) [30], in which a policy is trained to imitate the actions in the dataset through  
829 supervised learning. While this is a simple approach, it has proved incredibly effective for robotic  
830 manipulation [29, 31, 32, 33, 34, 35, 36, 37], particularly when coupled with a large number of  
831 demonstrations [10, 20, 38, 39]. Concurrent work has proposed leveraging Diffusion Models [75] to  
832 train policies via BC [76] in order to handle multi-modality of demonstrations. Our work instead  
833 focuses on how to best imitate TAMP with Transformers; Diffusion Policies, in particular their  
834 Transformer variants, could be straightforwardly integrated into OPTIMUS.

835 Human supervision is a common source of demonstrations. Several prior works use kinesthetic  
836 teaching [77, 78, 79, 80], in which a human manually guides an arm through a task, but this does not  
837 scale. Many works have leveraged teleoperation systems [13, 14, 15, 20, 35, 38, 39, 81, 82, 83], in  
838 which a human remote controls a robot arm to guide it through a task. However, scaling teleoperation  
839 is costly because it can require months of data collection and numerous human operators [10, 20, 81].  
840 This has motivated the development of intervention-based systems, in which humans provide smaller  
841 corrective behaviors to an agent [84, 85, 86, 87, 88, 89], enabling more sample-efficient learning and  
842 less operator burden. Instead of relying on human operators for supervision, we learn policies from  
843 demonstrations provided by a TAMP supervisor, which can generate large, diverse datasets without  
844 human supervision.

### 845 E.2 Transformers for Robot Control

846 Recent work explores the application of Transformers to controlling robot manipulators. Transformer-  
847 based policy architectures such as Gato [12], PerAct [40], VIMA [41], RT-1 [10], Dasari and Gupta  
848 [42], and Behavior Transformer [43] have demonstrated impressive results across a range of robotic  
849 manipulation tasks, yet make use of discretization of the input observations and output actions,  
850 limiting their applicability to tasks requiring precise manipulation. Additionally, PerAct [40] and  
851 VIMA [41] use abstracted actions to ease the learning burden at the cost of expressivity and execution  
852 speed. HiveFormer [67] is closest to our method in terms of architecture and training protocol  
853 but also assumes temporally-extended motion planner actions. As a result, these systems require  
854 privileged knowledge of the geometry of the environment to ensure safety. In contrast, OPTIMUS  
855 uses a Transformer architecture that is efficient to train and scale, fast-to-execute, consumes raw  
856 observations, and outputs low-level control actions.

### 857 E.3 Task and Motion Planning

858 Task and Motion Planning (TAMP) [27] addresses controlling a hybrid system through planning  
859 a sequence of discrete of manipulation types (*task planning*) realized through continuous motions  
860 (*motion planning*). TAMP approaches consume kinematic or dynamic models [44] of individual  
861 manipulation types and search over combining them in a manner that achieves a goal. Classically,  
862 these models are engineered; however, recently, they have been learned using methods such as  
863 Gaussian Processes [64] or Deep Neural Networks [65, 90, 91]. These mixed engineering-learning  
864 TAMP techniques can be quite effective, but they impose a strong human design bias, capping policy  
865 performance. Also, they are too computationally expensive to be run in real-time, preventing them  
866 from quickly reacting to new observations.

867 There has been recent interest in approaches that imitate planning [45, 46, 47]; however, these  
868 approaches generally focus on single-step motion generation. The exception is [28], which recently  
869 proposed an approach, Guided TAMP, that directly imitates TAMP. Our work builds on this direction  
870 in several ways. First, Guided TAMP primarily addresses control from privileged state, while we  
871 focus exclusively on visuomotor learning, which requires fewer assumptions. Second, Guided TAMP  
872 proposes a hierarchical policy that first predicts a discrete task-level action and then, conditioned on  
873 that action, predicts the next control. In order for the learner to predict a task-level action, they require  
874 a fixed set of ground actions, preventing the same policy from being deployed in tasks, for example,

875 with varying numbers of objects. In contrast, our Transformer architecture does not explicitly reason  
876 about task-level actions and thus does not require grounding and fixing the objects in the scene.  
877 Finally, we identify new considerations when using TAMP as a data generation pipeline.